

Chemical clocks and their time zones: understanding the $[s/Mg]$ –age relation with birth radii

Bridget Ratcliffe,¹★ Ivan Minchev,¹ Gabriele Cescutti,^{2,3,4} Emanuele Spitoni,³ Henrik Jönsson,⁵

Friedrich Anders,^{6,7,8} Anna Queiroz,^{1,9,10} Matthias Steinmetz¹

¹Leibniz-Institut für Astrophysik Potsdam (AIP), An der Sternwarte 16, 14482 Potsdam, Germany

²Dipartimento di Fisica, Sezione di Astronomia, Università di Trieste, via G. B. Tiepolo 11, 34143 Trieste, Italy

³INAF, Osservatorio Astronomico di Trieste, via G.B. Tiepolo 11, 34131, Trieste, Italy

⁴INFN, Sezione di Trieste, Via A. Valerio 2, I-34127 Trieste, Italy

⁵Materials Science and Applied Mathematics, Malmö University, SE-205 06 Malmö, Sweden

⁶Dept. de Física Quàntica i Astrofísica (FQA), Universitat de Barcelona (UB), C Martí i Franqués, 1, 08028 Barcelona, Spain

⁷Institut de Ciències del Cosmos (ICCUB), Universitat de Barcelona (UB), C Martí i Franqués, 1, 08028 Barcelona, Spain

⁸Institut d'Estudis Espacials de Catalunya (IEEC), C Gran Capità, 2-4, 08034 Barcelona, Spain

⁹Laboratório Interinstitucional de e-Astronomia - LIneA, Rua Gal. José Cristino 77, Rio de Janeiro, RJ - 20921-400, Brazil

¹⁰Institut für Physik und Astronomie, Universität Potsdam, Haus 28 Karl-Liebknecht-Str. 24/25, D-14476 Golm, Germany

Accepted XXX. Received YYY; in original form ZZZ

ABSTRACT

The relative enrichment of s-process to α -elements ($[s/\alpha]$) has been linked with age, providing a potentially useful avenue in exploring the Milky Way's chemical evolution. However, the age– $[s/\alpha]$ relationship is non-universal, with dependencies on metallicity and current location in the Galaxy. In this work, we examine these chemical clock tracers across birth radii (R_{birth}), recovering the inherent trends between the variables. We derive R_{birth} and explore the $[s/\alpha]$ –age– R_{birth} relationship for 36,652 APOGEE DR17 red giant and 24,467 GALAH DR3 main sequence turnoff and subgiant branch disk stars using $[Ce/Mg]$, $[Ba/Mg]$, and $[Y/Mg]$. We discover that the age– $[s/Mg]$ relation is strongly dependant on birth location in the Milky Way, with stars born in the inner disk having the weakest correlation. This is congruent with the Galaxy's initially weak, negative $[s/Mg]$ radial gradient, which becomes positive and steep with time. We show that the non-universal relations of chemical clocks is caused by their fundamental trends with R_{birth} over time, and suggest that the tight age– $[s/Mg]$ relation obtained with solar-like stars is due to similar R_{birth} for a given age. Our results are put into context with a Galactic chemical evolution model, where we demonstrate the need for data-driven nucleosynthetic yields.

Key words: Galaxy: abundances – Galaxy: evolution – Galaxy: disc – stars: abundances

1 INTRODUCTION

Chemical abundances are connected to a star's age and place of birth (Freeman & Bland-Hawthorn 2002; Ratcliffe et al. 2022), providing an effective tool in analyzing the Milky Way's evolutionary history. In particular, recent works have utilized the link between abundances and age to estimate stellar ages for large samples of red giant branch stars (Hayden et al. 2022; Ciucă et al. 2023; Leung et al. 2023; Anders et al. 2023), where traditional methods fail or only provide ages for small samples in select fields. While these abundance-driven ages have improved our understanding of important evolutionary events, some of the models can be quite complex, and may not capture the precise nature of the abundance–age relationship.

Over the past few years, the ratio between s-process and α -elements ($[s/\alpha]$) has been found to be linearly related with age in Milky Way solar-like stars (Nissen 2015; Nissen et al. 2020b) and giants (Slumstrup et al. 2017), as well as in other galaxies (Skúladóttir et al. 2019). Understanding this link between $[s/\alpha]$ and age could provide

a way to examine chemical evolution by omitting the dependencies in modeling age. The negative correlation between $[s/\alpha]$ and age is driven by the differing timescales to synthesize the two elements, as α -elements are created during supernovae II (SNII) which happen on fast timescales, while s-process elements are produced in the asymptotic giant branch (AGB) phase of low- and intermediate-mass stars which happens on a slower timescale (Karakas & Lattanzio 2014, Matteucci 2021 and references within). The relative differences in the timescales suggests the possibility that the $[s/\alpha]$ ¹ abundance can be an age indicator, or chemical clock (Nissen 2015; Tucci Maia et al. 2016; Spina et al. 2016).

Using only 25 solar-like stars, da Silva et al. (2012) found a correlation between $[s/\alpha]$ and age, which has successfully been replicated with more stars in other works using solar-type stars in the solar neighborhood (Nissen 2015, 2016; Tucci Maia et al. 2016; Titarenko et al. 2019; Nissen et al. 2020b; Jofré et al. 2020). However, its de-

¹ The most common chemical clock is $[Y/Mg]$ or $[Y/Al]$, though similar trends are found across other s-process and α -elements.

★ E-mail: bratcliffe@aip.de

pendency on location in the Galaxy (Casali et al. 2020; Casamiquela et al. 2021; Viscasillas Vázquez et al. 2022) and metallicity (Feltzing et al. 2017; Delgado Mena et al. 2017; Sales-Silva et al. 2022) is an ongoing question. Quantifying this radial dependency is a non-trivial task, as stars radially migrate away from their birth sites (Sellwood & Binney 2002; Roškar et al. 2008; Schönrich & Binney 2009; Minchev & Famaey 2010; Frankel et al. 2020), blurring fundamental chemical relations (e.g. Ratcliffe et al. 2023).

Recently, works have utilized the homogeneity of birth clusters (Bland-Hawthorn et al. 2010) to estimate stellar birth radii (R_{birth}) directly from their metallicities and ages. In order to assign a specific [Fe/H] and age to a birth location, the relationship between age, birth radius, and [Fe/H] over time needs to be known. While this relationship can be modeled (Frankel et al. 2018), more recent works have proposed methods which require less assumptions. In order to derive R_{birth} , Minchev et al. (2018) simultaneously recovered the metallicity evolution in the Galactic disk over time by enforcing the resulting R_{birth} distributions to remain physically meaningful. More recently, Lu et al. (2022) discovered a linear relation between the scatter in [Fe/H] for a given age and the [Fe/H] gradient evolution with time, allowing for the evolution of the metallicity gradient to be recovered with minimal assumptions. Applying this method to APOGEE DR17, Ratcliffe et al. (2023) derived R_{birth} for 145,447 red giant stars to recover the time evolution of chemical abundances across the Milky Way disk, revealing the information lost when only considering the radial gradient evolution estimated using current radius. That work put in context (and quantified) the expectation from models and simulations that radial mixing has significantly distorted present day chemo-kinematical relations used for inferring the Milky Way formation history (e.g. Pilkington et al. 2012; Minchev et al. 2012, 2014; Kubryk et al. 2013; Vincenzo & Kobayashi 2020).

In this work, we explore the universality of chemical clocks across birth radii for giants and main-sequence turnoff and subgiant branch (MSTO+SGB) disk stars. In particular, we examine how the age—[s/Mg] relationship differs across the Galaxy after minimizing the effect of radial migration. Section 2 presents the data sets used in this analysis. Section 3 gives the results and discussion of our findings in relation to previous works. Our conclusions are given in Section 4.

2 DATA

We examine three s-process elements — Ce, Ba, and Y — to study the relationship between [s/Mg], age, and birth radii. We use the [Ce/Fe] abundance from the BACCHUS Analysis of Weak Lines in APOGEE Spectra (BAWLAS; Hayes et al. 2022) catalog, and pair it with [Fe/H] and [Mg/Fe] abundances from APOGEE DR17 (Abdurro’uf et al. 2022; Majewski et al. 2017) of the fourth phase of the Sloan Digital Sky Survey (SDSS-IV; Blanton et al. 2017), which are processed using the APOGEE Stellar Parameter and Chemical Abundance Pipeline (ASPCAP; Holtzman et al. 2015; García Pérez et al. 2016; Jönsson et al. 2020). We partner these abundances with spectroscopic stellar ages from Anders et al. (2023) and guiding radii (R_{guide}) calculated as:

$$R_{\text{guide}} = R_{\text{gal}} V_{\phi} / V_0,$$

where V_{ϕ} and R_{gal} are the Galactocentric azimuthal velocity and Galactocentric cylindrical radius from the astroNN catalog (Leung & Bovy 2019), and $V_0 = 229.76$ km/s is the Milky Way rotation curve at solar radius (Bovy et al. 2012; Schönrich et al. 2010). To ensure that we select a high quality sample, we use APOGEE red giant ($2 < \log g < 3.6$, $4250 \leq T_{\text{eff}} \leq 5500$ K) disk ($|z| < 1$ kpc,

eccentricity < 0.5 , $|[\text{Fe}/\text{H}]| < 1$) stars with unflagged abundances, $[\text{Fe}/\text{H}]_{\text{err}} < 0.015$, $\text{age}_{\text{err}} < 1.5$ Gyr, $\text{SNR} > 100$, $\text{age} < 12$ Gyr, $|[\text{Ce}/\text{Fe}]| \leq 1$, and $[\text{Ce}/\text{Fe}]_{\text{err}} < 0.07$ dex.

We additionally use the [Y/Fe], [Ba/Fe], [Mg/Fe], and [Fe/H] abundance measurements provided in GALAH DR3 (Buder et al. 2021), with ages from the *STARHORSE* value-added catalog (Queiroz et al. 2023), which was recently corrected in a new version². R_{guide} is again calculated from cylindrical rotational velocity, with kinematics from the dynamics value-added catalog. For our GALAH MSTO+SGB disk ($|[\text{Fe}/\text{H}]| < 1$, eccentricity < 0.5 , $|z| < 1$ kpc) sample, we perform similar cuts as above; we keep stars with unflagged abundances, $|[\text{X}/\text{Fe}]| < 1$, $[\text{Fe}/\text{H}]_{\text{err}} < 0.1$, $\text{age}_{84-\text{age}_{16}} < 2.5$ Gyr, $\text{snr}_{\text{c2_iraf}} > 50$, $2 < \text{age} < 12$ Gyr, and $[\text{X}/\text{Fe}]_{\text{err}} < 0.1$ dex.

We estimate a star’s birth radius directly from their [Fe/H] and age measurements:

$$R_{\text{birth}}(\text{age}, [\text{Fe}/\text{H}]) = \frac{[\text{Fe}/\text{H}] - [\text{Fe}/\text{H}](R = 0, \tau)}{\nabla[\text{Fe}/\text{H}](\tau)}, \quad (1)$$

using the birth metallicity gradient ($\nabla[\text{Fe}/\text{H}](\tau)$) and central metallicity evolution over cosmic time τ ($[\text{Fe}/\text{H}](R = 0, \tau)$) from Ratcliffe et al. (2023) (see their section 3 for more information on the birth radii derivation). We correct for the 0.05 dex systematic offset in [Fe/H] between GALAH and APOGEE (Buder et al. 2021) before calculating R_{birth} for our GALAH sample. Since the main goal of this work is to look at overall trends with R_{birth} between [s/Mg] and age, and not to directly compare the numerical relationships between catalogs, we do not correct for other potential offsets. To get the [s/Mg] abundance, we simply subtract [Mg/Fe] from [s/Fe]. After performing the quality cuts listed above and removing stars with $R_{\text{birth}} < 0$, we are left with 36,652 APOGEE giants and 24,467 GALAH MSTO+SGB stars.

3 RESULTS AND DISCUSSION

With estimates of stellar ages and birth radii for large samples of stars, we can analyze the properties of chemical clocks over lookback time — which is not the same as age, see e.g. Ratcliffe et al. (2023) — and assess the effect of radial migration by comparing these properties to observed trends with guiding radii.

3.1 Radial gradient evolution

Using our R_{birth} estimates, we find distinct trends between [s/Mg] and R_{birth} in the top panels of Figure 1, where the R_{birth} –[s/Mg] relation illustrates the time evolution of [s/Mg] abundance gradients. In particular, we find that for all three of our [s/Mg] relations, the youngest mono-age populations have a steep positive radial gradient, while the oldest mono-aged populations have a weaker radial gradient. In fact, the three oldest age groups correspond to the high- α sequence (see Anders et al. 2023; Queiroz et al. 2023), which appear to have a slightly negative [s/Mg] radial birth gradient.

Once the low- α sequence began forming, the [s/Mg] radial gradient began quickly steepening with time. This steepening in the radial gradient visualized in the top panels of Figure 1 can be interpreted as a rapid increase in the enrichment with Galactic radius. This can be explained as an effect of radial migration, since the production of the s-process elements occurs during the AGB phase, which gives sufficient time for migration to proceed. The larger fraction of s-process

² <https://data.aip.de/projects/aqueiroz2023.html>

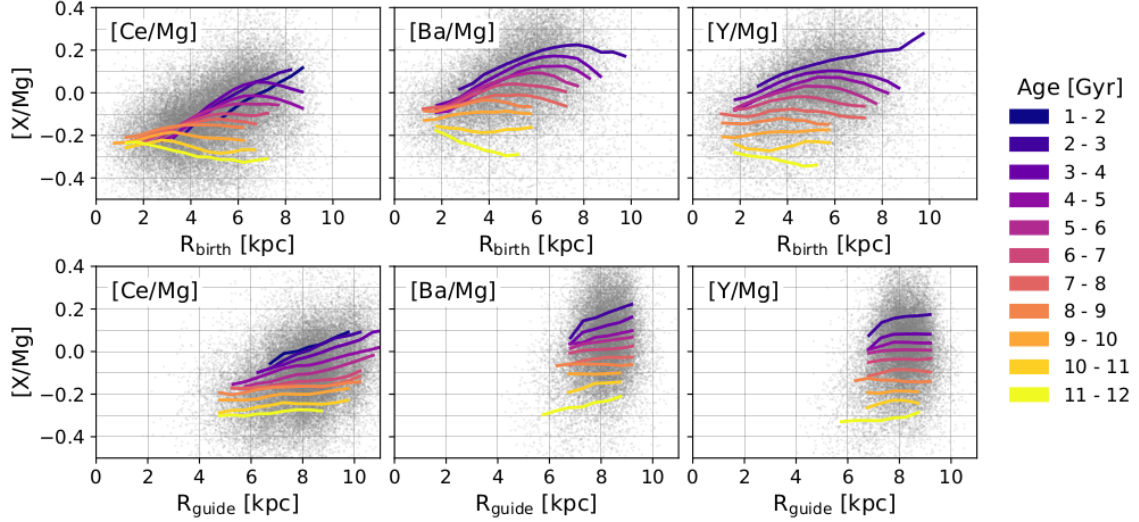


Figure 1. Time evolution of $[s/\text{Mg}]$ abundance gradients for our APOGEE ($[\text{Ce}/\text{Mg}]$) and GALAH ($[\text{Ba}/\text{Mg}]$, $[\text{Y}/\text{Mg}]$) samples. **Top:** Running means of different mono-age populations, determined by calculating the average $[s/\text{Mg}]$ for R_{birth} bins of width 0.5 kpc and then smoothed over 1 kpc. Note that age here becomes look-back time, since we are using R_{birth} . **Bottom:** Same as the top panels, but looking at the variation over age with R_{guide} . $[s/\text{Mg}]$ has a weak relationship with R_{birth} for older aged stars, which becomes positive and stronger with decreasing lookback time. The outer disk sees a faster enrichment in $[s/\text{Mg}]$ than the inner disk due to AGB stars migrating outwards before polluting the interstellar medium.

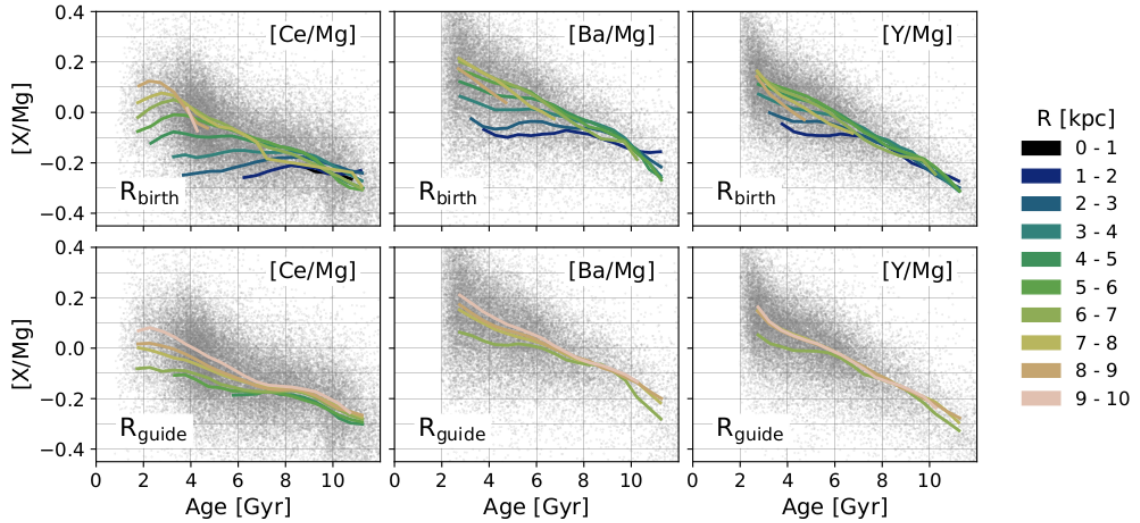


Figure 2. The age– $[s/\text{Mg}]$ plane of $[\text{Ce}/\text{Mg}]$ (APOGEE), $[\text{Ba}/\text{Mg}]$ (GALAH), and $[\text{Y}/\text{Mg}]$ (GALAH) overlaid by the running means of **top:** mono- R_{birth} populations and **bottom:** mono- R_{guide} populations. The running means are measured by calculating the average $[s/\text{Mg}]$ for age bins of 0.5 Gyr and smoothing over 1 Gyr. The smaller R_{birth} tracks show a weak relationship with age while the correlation between $[s/\text{Mg}]$ and age becomes quite strong for larger R_{birth} . Each R_{birth} sees a similar trend with $[s/\text{Mg}]$ over time; a radius sees an initial increase in $[s/\text{Mg}]$ until it flattens and stays nearly constant with time until the present day. This trend is drastically different than looking at mono- R_{guide} groups, which show minimal differences beyond slightly steeper slopes for outer radii.

elements at larger radius is then due to low- and intermediate-mass AGB stars migrating before polluting the interstellar medium. Indeed, it is well-established (Minchev et al. 2014; Frankel et al. 2020) that outside ~ 1 disk scale-length (~ 3.5 kpc; Bland-Hawthorn & Gerhard 2016), stars migrate larger distances outward and contribute more to a given radius. The steep $[s/\text{Mg}]$ radial gradient for the youngest populations also explains the scatter in $[s/\text{Mg}]$ found in young (< 2 Gyr) open clusters (Peña Suárez et al. 2018; Casali et al. 2020), as there is a range of $[s/\text{Mg}]$ values throughout the disk for a given (younger) age.

The bottom row of Figure 1 presents the R_{guide} – $[s/\text{Mg}]$ plane for

mono-age populations, illustrating the differences in measuring the radial $[s/\text{Mg}]$ gradients with R_{birth} (top row) and R_{guide} (bottom row). Similar to Ratcliffe et al. (2023), we find that the observed radial gradients with R_{guide} are weaker than the radial birth gradients, showing the level to which radial migration masks fundamental trends. Particularly for $[\text{Ba}/\text{Mg}]$ and $[\text{Y}/\text{Mg}]$ (GALAH sample), the R_{guide} – $[s/\text{Mg}]$ relation has a minor correlation overall. $[\text{Ce}/\text{Mg}]$ (APOGEE sample) shows similar trends, however due to the larger spatial coverage, the younger aged populations show a positive radial slope which is only hinted at in the GALAH sample.

3.2 Enrichment with cosmic time

While the $[s/\text{Mg}]$ radial gradient can provide insights into how the relative fraction of s-process to α -elements varies across the disk with time, the age– $[s/\text{Mg}]$ relation is potentially a useful tool in estimating stellar age that needs better understanding. Previous works have found that the age– $[s/\alpha]$ relation changes as a function of current radius, suggesting that the differences arise from the strong, non-monotonic dependence of the s-process yields with metallicity and different star formation histories (Casali et al. 2020). However, due to radial mixing processes, a given location in the Galaxy is comprised of stars born in a range of Galactic radii (depending on the age; see, e.g. Minchev et al. 2018; Agertz et al. 2021).

The top panels of Figure 2 show the age– $[s/\text{Mg}]$ relation for stars born at different locations in the Galaxy. We find that most mono- R_{birth} populations increase in $[s/\text{Mg}]$ before flattening out and seeing minimal differences in $[s/\text{Mg}]$ at later times. The flattening occurs at increasingly younger age for larger radii, which can be linked to the disk inside-out growth. In our data sets, the larger R_{birth} bins do not show a weakening in the age– $[s/\text{Mg}]$ gradient due to the lack of younger stars. This trend is consistent across red giants ($[\text{Ce}/\text{Mg}]$) and MSTO+SGB stars ($[\text{Ba}/\text{Mg}]$, $[\text{Y}/\text{Mg}]$), and is in disagreement with previous work that found the age– $[s/\text{Mg}]$ relation to be weaker in field giants and stronger in dwarfs (Katime Santrich et al. 2022). This shows that once working with R_{birth} , the differences among different stellar evolutionary states is minimized. Given that each birth radius has a similar trend in enrichment of $[s/\text{Mg}]$, this suggests that the effect of star formation is simply to shift the trends to larger radii as the disk grows with time.

In contrast to the top panels of Figure 2, the bottom row shows the age– $[s/\text{Mg}]$ relation for stars in different guiding, rather than birth, radial bins. We find that the well-defined self-similar trends seen for the mono- R_{birth} populations are now strongly blurred and largely overlapping. In particular, the flattening for younger ages at a given radius is almost completely lost, especially for $[\text{Ba}/\text{Mg}]$ and $[\text{Y}/\text{Mg}]$, except for a hint in the innermost R_{guide} bin.

Using open clusters, Viscasillas Vázquez et al. (2022) found that $[\text{Ba}/\text{Mg}]$ and $[\text{Y}/\text{Mg}]$ have respectively a weak and inverted trend with age in the inner disk. Using birth radii, we find that both $[\text{Ba}/\text{Mg}]$ and $[\text{Y}/\text{Mg}]$ have a weakly positive relation with age for smaller R_{birth} . In fact, we find the mono- R_{birth} populations behave similarly for all 3 elements (albeit with different slopes) in the $[s/\text{Mg}]$ –age plane, which differs from previous findings reporting that $[\text{Y}/\text{Mg}]$ and $[\text{Ba}/\text{Mg}]$ have different trends (e.g. da Silva et al. 2012), and shows the additional information gained using birth radii. Recently, Casali et al. (2023) showed that stars located in outer regions of the disk lie on steeper slopes in the age– $[\text{Ce}/\alpha]$ plane than stars currently located more inwards. Our work agrees with this finding, with our Figure 1 illustrating that this is caused by a more intense enrichment of $[s/\text{Mg}]$ in the outer disk.

As mentioned in Section 3.1, the $[s/\text{Mg}]$ radial gradient has been strengthening with time. In both our GALAH and APOGEE samples, the valley between the high- and low- α sequences happens between 9 and 10 Gyr ago, suggesting that chemical clocks behave differently for the two sequences. The validity of chemical clock indicators using s-process elements in the high- α sequence has been questioned before, with arguments that AGB stars would not have produced enough s-process elements that quickly (Hayden et al. 2022). However, we see in Figure 2 that these older stars have the strongest correlation with age, showing minimal differences across the different mono- R_{birth} populations. This also contrasts the differences between using current and birth radius, as the age– $[s/\text{Mg}]$ relation has been found

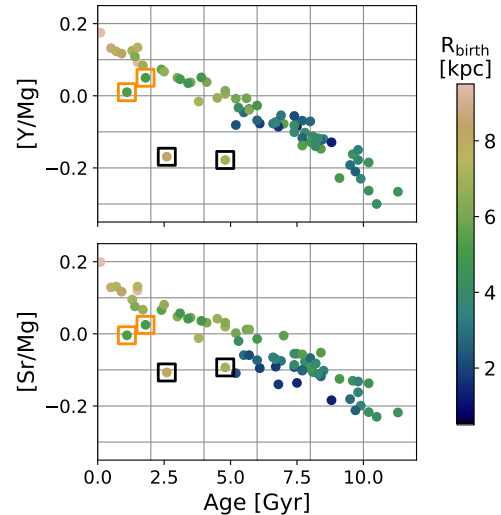


Figure 3. Top: The age– $[\text{Y}/\text{Mg}]$ and **bottom:** age– $[\text{Sr}/\text{Mg}]$ relation of 72 nearby solar-like stars presented by Nissen et al. (2020b). Stars are colored by their estimated R_{birth} . The linear $[\text{Y}/\text{Mg}]$ and $[\text{Sr}/\text{Mg}]$ relations with age results from stars with different R_{birth} across age, with the general trend of younger stars born at larger radii. The main deviants from this line (the components of ζ Retucili (black squares) and the two Na-rich stars (orange squares) are due to their differing birth location compared to other stars at a similar age. This figure illustrates that scatter about the chemical clock relation is a result of a sample containing stars born at different radii at a given age.

to be flat for older stars (Casali et al. 2023). One way to interpret this is that as the disk evolved, factors — such as radial migration processes — caused a variation in the production of $[s/\text{Mg}]$ as a function of radius, therefore creating a spread in $[s/\text{Mg}]$ abundance for a given age which increased with time. We explore these factors in Section 3.4 using Galactic chemical evolution modeling.

3.3 Tight age– $[s/\text{Mg}]$ relationship in solar twins is driven by varying birth radii

The tight relation between $[s/\text{Mg}]$ and age found for solar twins in e.g. Nissen (2015); Tucci Maia et al. (2016); Nissen et al. (2020b) led to the attempt of expanding this relation to larger samples. While some works have not found a metallicity dependence (Titarenko et al. 2019), others have noted a dependence on $[\text{Fe}/\text{H}]$ when examining larger regions of the Galaxy, suggesting that the linear relation between age and chemical clocks is limited by $[\text{Fe}/\text{H}]$ (Feltzing et al. 2017; Delgado Mena et al. 2019). For example, Casali et al. (2020) found that lower- $[\text{Fe}/\text{H}]$ stars had a higher correlation between $[\text{Y}/\alpha]$ and age, while the higher- $[\text{Fe}/\text{H}]$ stars had the weakest slope in the age– $[\text{Y}/\alpha]$ plane.

Since R_{birth} , $[\text{Fe}/\text{H}]$, and age are directly linked, it is natural that the differences across metallicity described above are potentially driven by varying R_{birth} . Indeed, for a given age, the higher- $[\text{Fe}/\text{H}]$ stars have smaller R_{birth} , which are the birth radii with the weakest age– $[s/\text{Mg}]$ relation. Another way to think of this is that the lower-metallicity stars come from a wider variety of R_{birth} (see the right panel of Figure 2 in Ratcliffe et al. 2023), and therefore run through more mono- R_{birth} populations in Figure 2 faster than the higher- $[\text{Fe}/\text{H}]$ stars. The dependency on $[\text{Fe}/\text{H}]$ therefore seems to be due to looking at stars born in different places of the Milky Way.

What does this mean for the samples of solar-like stars that show

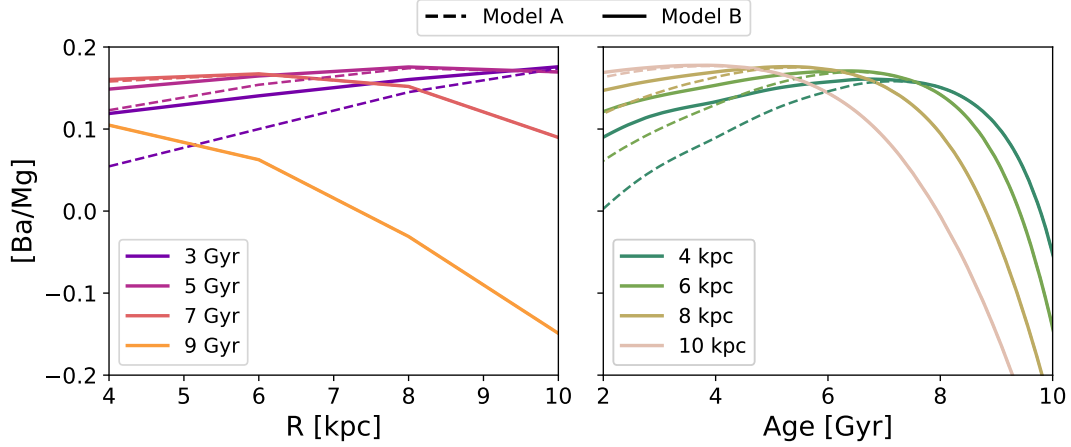


Figure 4. The left: $[\text{Ba}/\text{Mg}]$ vs R_{birth} and right: $[\text{Ba}/\text{Mg}]$ vs age planes using a single-infall GCE model with inside out growth and simple radial migration as described in Section 3.4 (Model A, dashed lines). Model A fails to reproduce the observed relationship between age, $[\text{Ba}/\text{Mg}]$, and R_{birth} . Particularly, the right panel shows that mono- R_{birth} populations see a decline in $[\text{Ba}/\text{Mg}]$ with decreasing age — unlike the trends shown in Figure 2. Model B (solid lines), which allows for more production of Ba at higher metallicities in AGB stars, corrects this issue, and is able to capture the overall trends observed with our R_{birth} .

tight relations between age and $[s/\text{Mg}]$? Figure 3 shows the age– $[\text{Y}/\text{Mg}]$ and age– $[\text{Sr}/\text{Mg}]$ planes for the 72 nearby solar-type stars provided in Nissen et al. (2020b), colored by their derived R_{birth} . It is clear that there is a gradient with R_{birth} in these planes for this sample, with younger stars having larger R_{birth} and older stars having lower R_{birth} . The minor scatter seen about the correlation is due to varying R_{birth} for a given age, which is caused by the variation in $[\text{Fe}/\text{H}]$ at that age. In other words, the variation in $[s/\text{Mg}]$ about the chemical clock relation at a given age is due to stars being born at different birth radii. This is especially apparent in $[\text{Sr}/\text{Mg}]$, which does not show as tight of a correlation with age as $[\text{Y}/\text{Mg}]$ does.

We find that the four stars that lie off of this tight relation particularly for $[\text{Y}/\text{Mg}]$ ($\zeta^1\text{Ret}$, $\zeta^2\text{Ret}$, and the Na-rich stars, marked with black and orange squares respectively) are born at predominantly different locations than the other stars with similar age in this sample.

3.4 Comparison with Galactic chemical evolution models

To interpret our results, we compare with the age– $[s/\text{Mg}]$ relationship produced using Galactic chemical evolution (GCE) modeling. We use the same nucleosynthesis adopted in the chemical evolution model by Van der Swaelmen et al. (2023) (model D), for what concerns magnesium and the r-process component of barium. The s-process component of barium is the same as assumed in Rizzuti et al. (2019), with the s-process production of AGB stars taken from the nucleosynthesis prescriptions of Cristallo et al. (2015) and those of massive stars from Frischknecht et al. (2016). The Galactic disk is described as rings of 2 kpc, with a single episode of infall following a decreasing exponential law with a fixed timescale of 5 Gyr, not varying with the galactic radius. These are simplified assumptions, compared to a possible double, or even triple, infall (see e.g. Spitoni et al. 2021, 2023) and also to the usual inside-out formation. The remaining parameters of chemical evolution such as initial mass function, star formation law, total surface mass density as a function of galactocentric distance and stellar lifetimes are the same as the disc phase considered in Cescutti et al. (2007). We use a single infall to naturally obtain a metallicity gradient flattening with time, as found in Lu et al. (2022) and Ratcliffe et al. (2023).

Unlike massive stars, AGB stars are long lived and thus have enough time to migrate and pollute neighboring bins. To account for this effect, we implement radial mixing in a simplified manner by assuming that at each time-step a fixed fraction of 10% of the barium in each ring is transferred to the ring outside. This mimics the enrichment by a percentage of AGB which migrates toward the outskirts of the disk, where they release their s-process enrichment; we define this as Model A.

The time evolution of the radial gradient of Model A is presented in the left panel of Figure 4 (dashed lines). This model captures the overall trend of the $[\text{Ba}/\text{Mg}]$ radial gradient across time that we find in Figure 1, i.e., the radial gradient begins negative and becomes positive with time. However, the age– $[\text{Ba}/\text{Mg}]$ relation for Model A (right panel of Figure 4, dashed lines) shows significant differences from our observational findings. This model predicts that after the initial pollution the $[\text{Ba}/\text{Mg}]$ abundance stays relatively constant with time for the outer radii, while in the inner disk its abundance significantly decreases (Figure 4). This is in strong disagreement with our results in Figure 2, where we find the $[\text{Ba}/\text{Mg}]$ abundance in the inner disk stays fairly constant with age and the outer disk sees a steep increase with time.

A possible explanation for the decrease in $[\text{Ba}/\text{Mg}]$ with time produced in Model A is that the amount of Ba produced in the models of high metallicity AGB stars is too low. To analyze this solution, we run Model A with a modification to the yields; the Ba yields for $Z > 0.01$ are replaced with the yields of $Z = 0.01$. In our set of nucleosynthesis, the yields of barium at $Z = 0.01$, are about a factor of 2 larger than the yields at $Z = 0.02$, depending on the mass of the AGB considered. The expectations of this modified model (Model B) are shown as the solid lines in Figure 4. We see that the discrepancies listed above are primarily resolved; that is, the $[\text{Ba}/\text{Mg}]$ abundance at each radius stays relatively constant with time after its initial increase. The results of Model B also appear to agree with what concerns the $[\text{Ba}/\text{Mg}]$ vs R_{birth} plot (solid lines in left panel of Figure 4), although in this plane the difference imposed by the variation in the yields are less significant. We underline that with our data it is not trivial to disentangle possible enrichment of s-process elements happening in binary systems. In this scenario, if the primary ended its life at AGB, the secondary star could be

enhanced in s-process elements; at the same time, the mass transfer can bias the determination of the age toward younger ages. Further investigations are needed to understand the impact of this population that at this stage we consider negligible.

The results that we found for $[\text{Ba}/\text{Mg}]$ can be explained by a disk with a decreasing exponential surface density and with a fixed infall timescale of 5 Gyr for all the radii, where the inner part enriches faster due to higher star formation efficiency, in an inside-out fashion. This combined with a strong metallicity dependence in the yields of s-process, with a mild modification of the most metal-rich tail, and with a migration of around 10% of the AGB products can explain the trends found in the data. The results of this section are robust to different values of this migration percentage, with a smaller/larger fraction causing smaller/larger variations in $[\text{s}/\text{Mg}]$ across R_{birth} for younger ages. Choosing the optimal fraction is nontrivial and outside the scope of this work. However, at least with these simplified assumptions, the migration needed is mild.

We acknowledge that the model does not perfectly reproduce the data as there are many parameters in modeling the Milky Way's evolution. Moreover, the choice of how to replace the higher metallicity yields is arbitrary. Still, the goal of this section is to show that this model is able to capture the main trends from Figures 1 and 2 and it provides us an interpretation of our results. This section also shows the power of R_{birth} , and how it can be used to constrain GCE models.

4 CONCLUSIONS

This work investigated the age– $[\text{s}/\text{Mg}]$ relation across R_{birth} using 36,652 APOGEE DR17 red giant disk stars and 24,467 GALAH DR3 MSTO+SGB disk stars. Previous works found variations in chemical clocks with current radius, however due to stars radially migrating away from their birth sites, these fundamental trends can be difficult to interpret. In this work, we explore the relative evolution of s-process and α -elements across time with birth radii. Our key findings are:

- The $[\text{s}/\text{Mg}]$ radial birth gradient for all three elements examined started initially weakly negative, flattened around the time of high- to low- α transition, and then became increasingly positive (or concave downwards) toward redshift zero (Figure 1).
- The age– $[\text{s}/\text{Mg}]$ relation varies across R_{birth} , with each radius seeing an initial increase in $[\text{s}/\text{Mg}]$ before varying little with time (Figure 2). This suggests that the scatter about the $[\text{s}/\text{Mg}]$ –age line is predominantly due to samples containing a variety of R_{birth} for a given age.
- When the dispersion in R_{birth} is small for a given age (such as in Milky Way solar-like stars), a tight correlation between $[\text{s}/\text{Mg}]$ and age is found (Figure 3).
- Using a GCE model with standard nucleosynthetic yields, we find that the $[\text{Ba}/\text{Mg}]$ abundance decreases with time for each mono- R_{birth} population in disagreement with the data. A simple correction for allowing more Ba to be produced at higher metallicities, as well as a simple model of radial migration, address this issue and is able to reproduce the trends found using our R_{birth} estimates (Figure 4).

Our results explicitly show that there is no universal $[\text{s}/\text{Mg}]$ –age relation across the Galactic disk, in agreement with previous works (e.g. [Viscasillas Vázquez et al. 2022](#)). Here, however, we revealed how this correlation depends on R_{birth} (and thus $[\text{Fe}/\text{H}]$), which demonstrates the inherent relationship between $[\text{s}/\text{Mg}]$ abundance and age in the Milky Way that is not masked by radial migration. In particular, we illustrate how radial migration affects the $[\text{s}/\text{Mg}]$ radial gradient with time, which in turn creates a variation in the

$[\text{s}/\text{Mg}]$ abundance across birth radii and causes a weaker correlation between age and $[\text{s}/\text{Mg}]$ for younger ages.

The time evolution of the age– $[\text{s}/\text{Mg}]$ relation that we uncovered with knowledge of birth radius was used to constrain the metallicity dependence of the AGB yields, and the radial migration strength of a simple GCE model — which is typically constrained by only present-day observations with age and radius — and highlights the utility of R_{birth} in understanding the Milky Way's chemical evolution.

ACKNOWLEDGEMENTS

B.R. and I.M. acknowledge support by the Deutsche Forschungsgemeinschaft under the grant MI 2009/2-1. This work was also partially supported by the European Union (ChETEC-INFRA, project no. 101008324)

DATA AVAILABILITY

The datasets used and analysed for this study are derived from data released by APOGEE DR17, GALAH DR3, [Queiroz et al. \(2023\)](#) (corrected version: <https://data.aip.de/projects/aqueiroz2023.html>), [Anders et al. \(2023\)](#), and [Nissen et al. \(2020b\)](#) ([Nissen et al. 2020a](#)). The rest of the relevant datasets are available from the corresponding author on reasonable request.

REFERENCES

- Abdurro'uf et al., 2022, *ApJS*, 259, 35
 Agertz O., et al., 2021, *MNRAS*, 503, 5826
 Anders F., et al., 2023, *arXiv e-prints*, p. arXiv:2304.08276
 Bland-Hawthorn J., Gerhard O., 2016, *ARA&A*, 54, 529
 Bland-Hawthorn J., Krumholz M. R., Freeman K., 2010, *ApJ*, 713, 166
 Blanton M. R., et al., 2017, *The Astronomical Journal*, 154, 28
 Bovy J., et al., 2012, *ApJ*, 759, 131
 Buder S., et al., 2021, *MNRAS*, 506, 150
 Casali G., et al., 2020, *A&A*, 639, A127
 Casali G., et al., 2023, *arXiv e-prints*, p. arXiv:2305.06396
 Casamiquela L., Castro-Ginard A., Anders F., Soubiran C., 2021, *A&A*, 654, A151
 Cescutti G., Matteucci F., François P., Chiappini C., 2007, *A&A*, 462, 943
 Ciucă I., et al., 2023, *MNRAS*,
 Cristallo S., Straniero O., Piersanti L., Gobrecht D., 2015, *ApJS*, 219, 40
 Delgado Mena E., Tsantaki M., Adibekyan V. Z., Sousa S. G., Santos N. C., González Hernández J. I., Israelian G., 2017, *A&A*, 606, A94
 Delgado Mena E., et al., 2019, *A&A*, 624, A78
 Feltzing S., Howes L. M., McMillan P. J., Stokutė E., 2017, *MNRAS*, 465, L109
 Frankel N., Rix H.-W., Ting Y.-S., Ness M., Hogg D. W., 2018, *ApJ*, 865, 96
 Frankel N., Sanders J., Ting Y.-S., Rix H.-W., 2020, *ApJ*, 896, 15
 Freeman K., Bland-Hawthorn J., 2002, *ARA&A*, 40, 487
 Frischknecht U., et al., 2016, *MNRAS*, 456, 1803
 García Pérez A. E., et al., 2016, *AJ*, 151, 144
 Hayden M. R., et al., 2022, *MNRAS*, 517, 5325
 Hayes C. R., et al., 2022, *ApJS*, 262, 34
 Holtzman J. A., et al., 2015, *AJ*, 150, 148
 Jofré P., Jackson H., Tucci Maia M., 2020, *A&A*, 633, L9
 Jönsson H., et al., 2020, *AJ*, 160, 120
 Karakas A. I., Lattanzio J. C., 2014, *Publ. Astron. Soc. Australia*, 31, e030
 Katime Santrich O. J., Kerber L., Abuchaim Y., Gonçalves G., 2022, *MNRAS*, 514, 4816
 Kubryk M., Prantzos N., Athanassoula E., 2013, *MNRAS*, 436, 1479
 Leung H. W., Bovy J., 2019, *MNRAS*, 483, 3255
 Leung H. W., Bovy J., Mackereth J. T., Miglio A., 2023, *MNRAS*, 522, 4577

- Lu Y., Minchev I., Buck T., Khoperskov S., Steinmetz M., Libeskind N., Cescutti G., Freeman K. C., 2022, arXiv e-prints, p. [arXiv:2212.04515](#)
- Majewski S. R., et al., 2017, *AJ*, **154**, 94
- Matteucci F., 2021, *A&ARv*, **29**, 5
- Minchev I., Famaey B., 2010, *ApJ*, **722**, 112
- Minchev I., Famaey B., Quillen A. C., Dehnen W., Martig M., Siebert A., 2012, *A&A*, **548**, A127
- Minchev I., Chiappini C., Martig M., 2014, *A&A*, **572**, A92
- Minchev I., et al., 2018, *MNRAS*, **481**, 1645
- Nissen P. E., 2015, *A&A*, **579**, A52
- Nissen P. E., 2016, *A&A*, **593**, A65
- Nissen P. E., Christensen-Dalsgaard J., Mosumgaard J. R., Silva Aguirre V., Spitoni E., Verma K., 2020a, *VizieR Online Data Catalog*, pp [J/A+A/640/A81](#)
- Nissen P. E., Christensen-Dalsgaard J., Mosumgaard J. R., Silva Aguirre V., Spitoni E., Verma K., 2020b, *A&A*, **640**, A81
- Peña Suárez V. J., Sales Silva J. V., Katime Santrich O. J., Drake N. A., Pereira C. B., 2018, *ApJ*, **854**, 184
- Pilkington K., et al., 2012, *A&A*, **540**, A56
- Queiroz A. B. A., et al., 2023, *A&A*, **673**, A155
- Ratcliffe B. L., Ness M. K., Buck T., Johnston K. V., Sen B., Beraldo e Silva L., Debattista V. P., 2022, *ApJ*, **924**, 60
- Ratcliffe B., et al., 2023, *MNRAS*,
- Rizzuti F., Cescutti G., Matteucci F., Chieffi A., Hirschi R., Limongi M., 2019, *MNRAS*, **489**, 5244
- Roškar R., Debattista V. P., Quinn T. R., Stinson G. S., Wadsley J., 2008, *ApJ*, **684**, L79
- Sales-Silva J. V., et al., 2022, *ApJ*, **926**, 154
- Schönrich R., Binney J., 2009, *MNRAS*, **399**, 1145
- Schönrich R., Binney J., Dehnen W., 2010, *MNRAS*, **403**, 1829
- Sellwood J. A., Binney J. J., 2002, *MNRAS*, **336**, 785
- Skúladóttir Á., Hansen C. J., Salvadori S., Choplin A., 2019, *A&A*, **631**, A171
- Slumstrup D., Grundahl F., Brogaard K., Thygesen A. O., Nissen P. E., Jessen-Hansen J., Van Eylen V., Pedersen M. G., 2017, *A&A*, **604**, L8
- Spina L., Meléndez J., Karakas A. I., Ramírez I., Monroe T. R., Asplund M., Yong D., 2016, *A&A*, **593**, A125
- Spitoni E., et al., 2021, *A&A*, **647**, A73
- Spitoni E., et al., 2023, *A&A*, **670**, A109
- Titarenko A., Recio-Blanco A., de Laverny P., Hayden M., Guiglion G., 2019, *A&A*, **622**, A59
- Tucci Maia M., Ramírez I., Meléndez J., Bedell M., Bean J. L., Asplund M., 2016, *A&A*, **590**, A32
- Van der Swaelmen M., et al., 2023, *A&A*, **670**, A129
- Vincenzo F., Kobayashi C., 2020, *MNRAS*, **496**, 80
- Viscasillas Vázquez C., et al., 2022, *A&A*, **660**, A135
- da Silva R., Porto de Mello G. F., Milone A. C., da Silva L., Ribeiro L. S., Rocha-Pinto H. J., 2012, *A&A*, **542**, A84

This paper has been typeset from a $\text{\TeX}/\text{\LaTeX}$ file prepared by the author.